Received September 21, 2017, accepted October 22, 2017, date of publication November 8, 2017, date of current version December 5, 2017.

Digital Object Identifier 10.1109/ACCESS.2017.2771527

Sensitivity Analysis for the Power Quality Indices of Standalone PV Systems

DIONISIS VOGLITSIS[1], (Student Member, IEEE), NICK P. PAPANIKOLAOU[1], (Senior Member, IEEE), CHRISTOS A. CHRISTODOULOU[2], DIMITRIS K. BAROS[1], (Student Member, IEEE), AND IOANNIS F. GONOS[3], (Senior Member, IEEE)

[1]Electrical and Computer Engineering Department, Democritus University of Thrace, 67132 Xanthi, Greece
[2]Hellenic Distribution Network Operator S.A., 11743 Athens, Greece
[3]School of Electrical and Computer Engineering, National Technical University of Athens, 15780 Athens, Greece

Corresponding author: Nick P. Papanikolaou (npapanik@ee.duth.gr)

ABSTRACT Standalone photovoltaic systems is a key technology for the increase of renewable energy sources share in electricity production worldwide. The power quality of those systems plays a fundamental role in avoiding volatile power supply. This calls for a concrete design in order to meet power quality specifications. In this context, a methodology has been developed in a previous work, in order to set the values of the parameters that optimize the power quality indices of the system. In this paper, an extensive sensitivity analysis is performed regarding the influence of the optimized parameters variation on the power quality indices. Throughout the outcomes of the sensitivity analysis a more insightful view of the system performance under the deviations of system parameters is revealed, which in combination with the aforementioned optimal design strategy becomes an essential tool that ensures high power quality level. The theoretical outcomes are validated by experimental results, highlighting the effectiveness of the proposed design strategy.

INDEX TERMS Genetic algorithms, inverters, photovoltaic systems, power quality.

I. INTRODUCTION

During the past years Power Corporation Companies encourage the installation of standalone residential photovoltaic (PV) systems, by providing various motivations to the consumers, in order to meet both financial and ecological targets. The progress in the generation of electric energy by solar as well as the feed in tariffs and transaction policies of the emerging energy market, have turned PV-systems into a critical part of electrical networks [1]–[6]. The development of the standalone PV systems relies on their power quality, obliged to cope with the increasing demands of the consumers and the complexity of the modern electrical installations [7]–[9]. For these reasons, the design of a standalone PV system should comply with national and international power quality and safety standards. Complying with these standards ensures high power quality, secures power supply, safeguards people and infrastructures from accidents and moderates the initial and operational costs. Moreover, overdimensioning of the equipment should be avoided, taking into consideration techno-economical restrictions.

Although various techniques have been developed and implemented for the improvement of the power quality of standalone systems (e.g. load demand management [10]–[15], and supply voltage control using sophisticated control loops [16]–[20]), the initial design of the system is still the dominant factor. Inefficient selection of critical components may result in non-efficient operation of the standalone system, leading to expensive and non-practical topologies.

In order to meet the above demands and limitations, critical parameters of the PV system should be properly selected. As such, a constrained optimization problem is formed. Genetic algorithms are considered as robust, stochastic and heuristic optimization methods that give excellent results in several optimization problems [21], [22]. A genetic algorithm relies on processes of biological reproduction, crossover, and mutation to reach the global or ‘‘near-global’’ optimum. Usually, an initial population is provided, which is represented by bit strings that evolve randomization through successive generations in order to obtain an optimum for a particular fitness-function. Solutions with high suitability are mated with other solutions by crossing over parts of solution strings. Strings may also mutate. Solutions with poor fitness are improved by crossover using highly fit solutions.

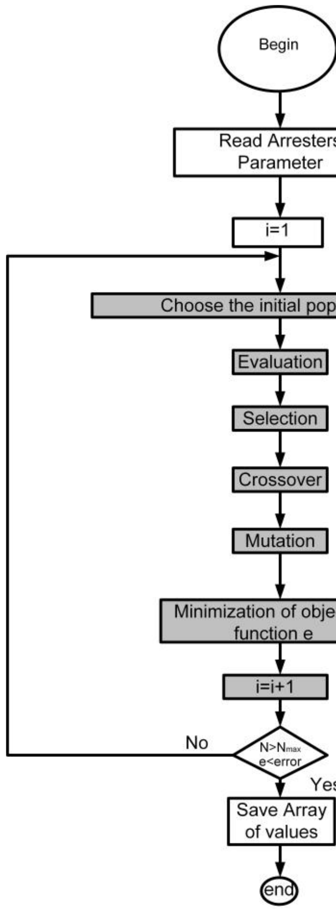

FIGURE 1. Genetic algorithm flowchart [21].

In this context, a genetic algorithm has been proposed in previous works [23]–[25] that optimizes the power quality of three-phase standalone PV residential systems; its flowchart is depicted in Fig. 1.

In the current work, power quality is expressed in terms of appropriate indices that incorporate the limitations of the relevant standards as well as practical dimensioning issues, avoiding so nonrealistic configurations. In this context, the proposed methodology [23] adjusts key variables (i.e. C_f, L_f, n, V_{dc}) of the standalone installation optimizing the following power indices; *asym*; THD_v; *sci*; *scs*; *nomi*, and reassuring the compliance of the power quality indices with predefined targets. This "initial design" approach takes a more comprehensive view of the autonomous system, ensuring the compliance of the defined indices with the demands of the International Standards and the common practice. In contrast to other methodologies [7], [26] that focus on reformative actions in an effort to align with the power quality demands, the algorithm presented in [23] proposes preventive actions in order to avoid the exceedance of the techno-economical restrictions.

Despite the fact that the proposed methodology adds flexibility to the design of standalone PV systems, the theoretical predictions may not always be verified due to a series of factors; the deviation between the nominal theoretical and the real values of the system components (i.e. capacitance, inductance, transformer ratio); the variation of the voltage level; and the variation of the load demand, are the main reasons for the above mismatch. As a result, the optimized solution may be proven insufficient under real operating conditions, failing to preserve the expected level of power quality. This in turns may have impact on the safe operation of the standalone installation. Hence, the optimal design has to be extensively assessed in terms of the expected deviations of the system parameters. In the current work the optimal design of standalone PV-installations presented in [23] is thoroughly investigated by means of an exhaustive sensitivity analysis, revealing the impact of each parameter on the power quality of the standalone system. The analysis reveals the effect of every system parameter on the power quality indices, as well as the tolerance of the optimized solution under real operating conditions. Thus, the main outcome of the current work is the enhancement of the design methodology of [23] by providing a comprehensive design of standalone PV systems that takes into consideration any possible parameter deviation. Additionality, experimental results validate the effectiveness of the proposed methodology.

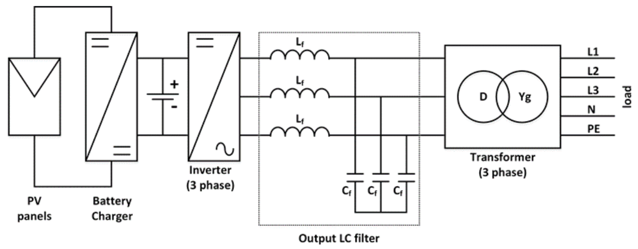

FIGURE 2. Configuration of the standalone PV system under study.

II. BASIC SYSTEM ANALYSIS

Fig. 2 depicts the block diagram of the standalone PV system under study. The main parts of the PV installation are [23]:

- the PV unit
- the series charger (DC/DC converter)
- the battery bank
- the three-phase inverter (H-bridge)
- the LC filter
- the three-phase transformer (Ygd connection).

The power quality indices are summarized as follows:

- Asymmetry due to single phase loads (*asym*); *asym* should not exceed 5%, according to [27]–[33]. According to the symmetrical components analysis of the system, *asym* is expressed by the following equation [23]:

$$\mathrm{asym} = \frac{V_2}{V_1}\cdot 100\% = \left\langle \begin{array}{l} \left\{1+\left[\left(\frac{f_r}{f_b}\right)^2-1\right]\frac{n^2R_L}{X_{Cf}}\tan[\arccos(pf)]\right\}^2 \\ +\left\{\left[\left(\frac{f_r}{f_b}\right)^2-1\right]\frac{n^2R_L}{X_{Cf}}\right\}^2 \end{array}\right\rangle^{-\frac{1}{2}} \cdot 100\% \quad (1)$$

- Total Harmonic Distortion at the load side (THD_V), calculated by using the symmetrical components analysis; THD_V should not be higher than 8%, according to [34]. According to the harmonic analysis of the system, THD_V is expressed by the following equation [23]:

$$\mathrm{THD_V} = \frac{1}{\mathrm{V_b}}\left\{\sum_{\mathrm{i}=3,5,\ldots} \mathrm{V}^2_{\mathrm{i(TP)}}\right\}^{1/2} \tag{2.1}$$

$$\mathrm{V_{i\,(TP)}} = \mathrm{V_{2,i}} = \mathrm{Z_{2,i}I_i} \tag{2.2}$$

$$\mathrm{Z_{2,i}} = 3\mathrm{n}^{-2}\frac{\mathrm{X_{Cf}}}{\left[\mathrm{i}-\frac{1}{\mathrm{i}}\left(\frac{\mathrm{f_r}}{\mathrm{f_b}}\right)^2\right]}, \tag{2.3}$$

where I_i is the rms value of the i-order load current harmonic component (per phase).

- Inverter Short Circuit Current Ratio (*sci*), denoting the short circuit current that both the inverter and the filter inductor have to withstand; *sci* should be less than 5, according to techno-economic constraints [23].
- Inverter Nominal Power Ratio (*scs*); it is a techno-economical factor which defines the necessary inverter over-dimensioning in order to meet the power quality targets and the inverter safe operation restrictions; *scs* should not exceed 2, according to techno-economic constraints [23].
- Inverter Nominal Current Ratio (*nomi*), denoting the maximum permissible capacitive current in the circuit; *nomi* should not exceed 1.5, according to techno-economic constraints [23].

The system parameters (f, q, n, V_{dc}) have been defined according to [23], as follows:

$$f = \frac{f_r}{f_b} \tag{3}$$

$$q = \frac{n^2 R_L}{X_{Cf}} \tag{4}$$

$$f_r = \frac{1}{2\pi\sqrt{L_f C_f}}, \tag{5}$$

where R_L, the (per phase) real component of the load equivalent impedance;

f_r, the filter resonant frequency;

$f_b = \omega_b/2\pi$, the fundamental frequency;

n, the three phase transformer turns ratio;

X_{Cf}, the filter capacitor impedance per phase (at fundamental frequency);

V_{dc}, the dc voltage at the inverter dc-side.

The above presented power quality indices are inserted into an objective function which expression is [23]:

$$\mathrm{e(k)} = \frac{\mathrm{asym}}{\mathrm{w_1}} + \frac{\mathrm{t_5}}{\mathrm{w_2}} + \frac{\mathrm{t_7}}{\mathrm{w_3}} + \frac{\mathrm{t_{11}}}{\mathrm{w_4}} + \frac{\mathrm{sci}}{\mathrm{w_5}} + \frac{\mathrm{scs}}{\mathrm{w_6}} + \frac{\mathrm{nomi}}{\mathrm{w_7}}, \tag{6}$$

where $w_{1,2\ldots,7}$ are weight factors, set by the maximum permissible values of the power quality indices [23], and

$$\mathrm{t_i} = \frac{\mathrm{X \cdot Z_i \cdot I_i}}{230}, \tag{7}$$

where $i = 5, 7, 11$ (the harmonic order).

According to [23], t_5, t_7 and t_{11} are computed considering X non-linear loads with harmonic current content equal to the maximum permissible limits for each harmonic component, according to IEC 61000-3-2 standard [35]. Hence, (6) is minimized through the genetic algorithm presented in Fig.1.

In the current analysis, the above indices as well as the amplitude modulation ratio of the SPWM controller (m_a) are analyzed with respect to the system parameters (n, V_{dc}) and the following variables:

- the filter inductance per line, L_f, extracted by (3)-(5):

$$L_f = \frac{qn^2 R_L}{\omega_b f^2} \tag{8}$$

- the filter capacitance per phase, C_f, extracted by (3)-(5):

$$C_f = \frac{1}{qn^2 R_L \omega_b} \tag{9}$$

Finally, by simple circuit analysis, R_L is given by the following equation:

$$R_L = \frac{(V_{2N} pf)^2}{P_L}, \tag{10}$$

where *pf* the load power factor; V_{2N}, the transformer line-to-line nominal secondary rms voltage value; and P_L, the load active power.

III. SENSITIVITY ANALYSIS

A sensitivity analysis is performed in order to investigate the influence of the above-mentioned parameters on the power quality indices. Previous works [23], [24] indicate that the compliance of the aforementioned power quality indices with the demanded limitations (according to international standards and techno-economical restrictions) depends on the appropriate selection of the system parameters values; these values are optimally selected by using an appropriate methodology, based on an artificial intelligence technique (i.e. a genetic algorithm). However, some power quality indices may still exceed their predetermined limits, due to the fact that the optimal values of the system parameters are not always attainable (for practical reasons). It is noted that even if the optimal parameters values are attainable these are about to alter in real life operation, being subjected to various operational and environmental factors such as voltage and current stresses, environmental conditions etc.

The sensitivity analysis reveals the behavior of each power quality index, indicating the influence of the parameters variation to the quality of the supplied power. The current work examines the dependence of the power quality indices (*asym*, THD_v, *sci*, *scs*, *nomi*) and m_a on the variations of C_f, L_f, n and V_{dc}, considering three different power levels for the standalone system, i.e. 1 kW, 20 kW and 50 kW. It is noted that the case of 1 kW is considered only for the -under scale-experimental evaluation of the theoretical calculations - presented in Section 4. Table 1 presents the optimal values of the aforementioned parameters for various X-values, obtained by

TABLE 1. Optimal parameters values calculated According to [32].

Power level	X	C_f (mF)	L_f (mH)	n	V_{dc} (V)
1 kW	0.3	0.398	5.32	0.510	300
	1	8.193	0.246	0.500	300
	3	9.419	0.234	0.500	300
20 kW	5	10.347	0.226	0.500	300
	7	11.188	0.220	0.500	300
	9	11.849	0.214	0.500	300
	1	6.687	0.278	0.834	557
	3	10.41	0.180	0.672	450
50 kW	5	6.584	0.312	0.913	596
	7	7.488	0.281	0.881	571
	9	9.935	0.219	0.785	503

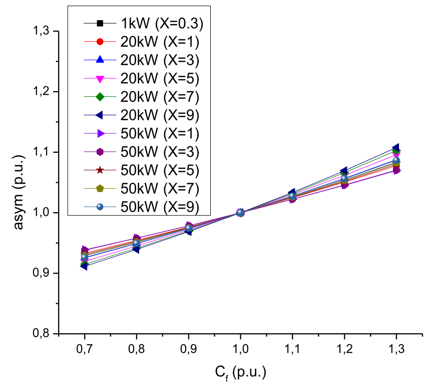

FIGURE 3. *asym* vs C_f.

the methodology presented in [23] and taking under consideration the restrictions defined in Section II. It is noted that if the harmonic content of the load is lower than the aforementioned limits, then X becomes lower than unity. On the other hand, Table 2 presents the values of the power quality indices, calculated using the variables in Table I and according to the methodology in [23]. It is noted that the sensitivity analysis outcomes are normalized prior to the values in Tables 1 and 2, in order to perform reliable comparisons for all the scenarios under study (nominal load, V_{dc} range, X, etc).

TABLE 2. Estimated power quality indices (using the parameters values of Table1).

Power level	X	*asym*	m_a	THD_V	*sci*	*scs*	*nomi*
1 kW	0.3	5.779	0.538	3.887	4.677	1.059	1.205
	1	5.489	0.530	0.662	4.495	1.058	1.195
	3	5.349	0.517	1.695	4.520	1.156	1.339
20 kW	5	5.272	0.507	2.540	4.211	1.233	1.456
	7	5.206	0.499	3.259	3.959	1.305	1.568
	9	5.122	0.492	3.935	3.800	1.364	1.658
	1	5.480	0.486	0.297	5.308	1.006	1.115
	3	5.475	0.483	0.880	5.274	1.011	1.122
50 kW	5	5.262	0.483	1.230	4.867	1.107	1.262
	7	5.126	0.482	1.617	4.754	1.152	1.324
	9	5.078	0.482	1.960	4.452	1.193	1.386

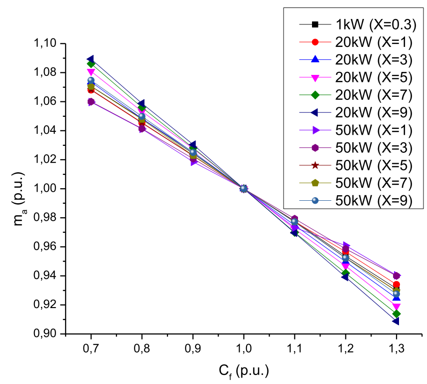

FIGURE 4. m_a vs C_f.

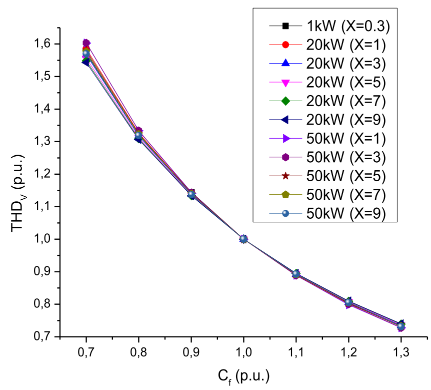

FIGURE 5. THD_V vs C_f.

The outcomes of the sensitivity analysis are summarized in Figs. 3-22, where the variations of the examined power quality indices are illustrated as a function of the system parameters. In more details, Figs. 3-8 illustrate *asym*, m_a, THD_v, *sci*, *scs*, and *nomi* as functions of C_f considering the power levels and X-values of Table 1. The same parameters are depicted as functions of L_f, in Figs. 9-14. Finally, Figs. 15-20 present the abovementioned parameters as functions of n, whereas Figs. 21 and 22 highlight the effect of V_{dc} on *asym*, THD_V, *sci*, *scs*, *nomi*, PF_{inv}, and m_a. Several observations and conclusions are made, based on the presented sensitivity analysis results. To begin with, one may note that the load nominal power and the X-value do not have significant impact on power quality; this can be attributed to the initial optimal design that deflates the influence of those parameters. On the other hand, according to Figs. 3, 6, and 7, *asym*, *scs* and *nomi* depend strongly on the variation of C_f. Furthermore, Figs. 4-6 highlight that m_a, THD_V and *sci* are inversely correlated with C_f. In more details, even though the reduction of C_f has a positive impact on *asym* value (it slightly decreases), THD_V and *sci* deteriorate significantly and so there is a danger of exceeding their upper limits. This is

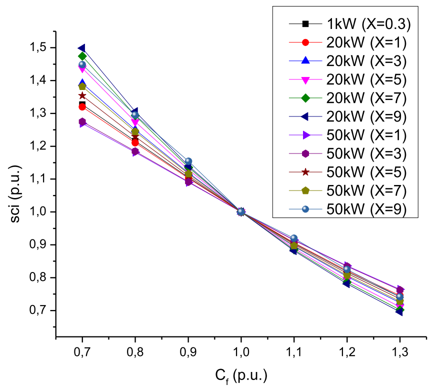

FIGURE 6. ***sci*** **vs** C_f**.**

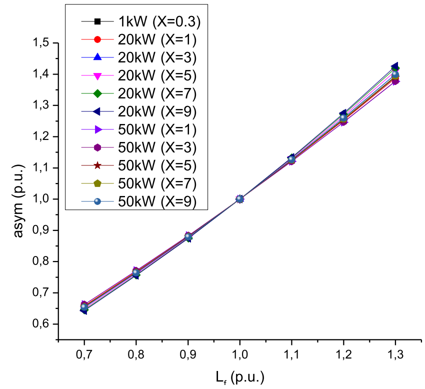

FIGURE 9. ***asym*** **vs** L_f**.**

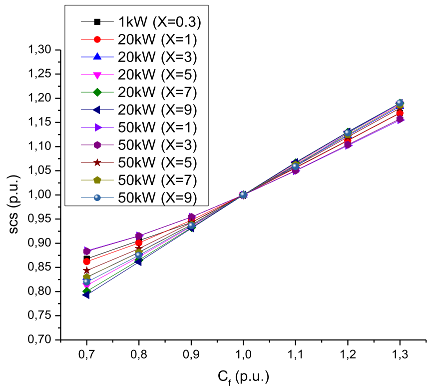

FIGURE 7. ***scs*** **vs** C_f**.**

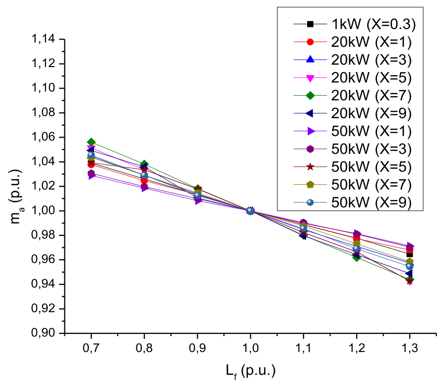

FIGURE 10. m_a **vs** L_f**.**

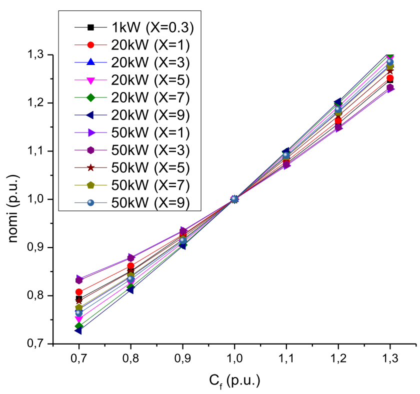

FIGURE 8. ***nomi*** **vs** C_f**.**

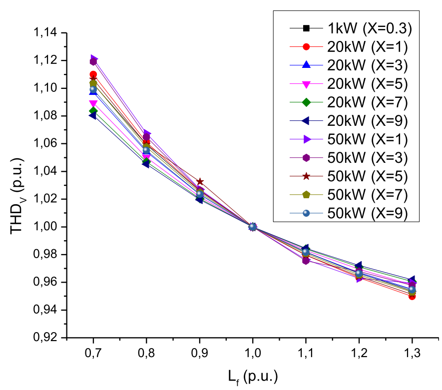

FIGURE 11. THD_V **vs** L_f**.**

due to the fact that the rms current value of C_f also decreases, calling for significantly higher reactive current amounts at the inverter output stage (in order to cover the lack of reactive power). As far as the influence of L_f concerns, Fig. 9 outlines that *asym* deviations are proportional to L_f ones, whereas all the other power quality indices, except *nomi*, are inversely proportional to L_f (according to Figs. 10-14). As Fig. 14 depicts, *nomi* has no dependence on L_f variations because it represents the ratio of the capacitive filter current part. The transformer turns ratio also affects the behavior of the power quality indices; in Figs. 15, 17, *asym* and THD_V are inversely correlated with *n*, whereas in Figs. 16, 19, and 20, m_a, *scs* and *nomi* increase as *n* rises. Nevertheless, among all other parameters, *n* is less possible to present significant alterations. Finally, as it is shown in Figs. 21, 22, V_{dc} influences only m_a, having no impact on the other indices.

The sensitivity analysis has highlighted the fact that the final design of the system has to take into account future alterations due to various operational / environmental conditions. Although it is proven that the optimal design methodology

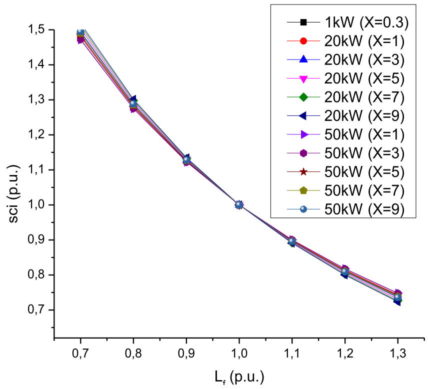

FIGURE 12. *sci* vs L_f.

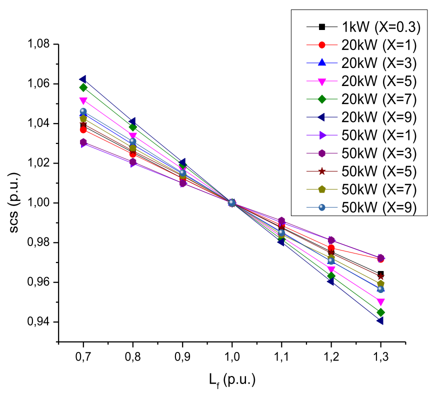

FIGURE 13. *scs* vs L_f.

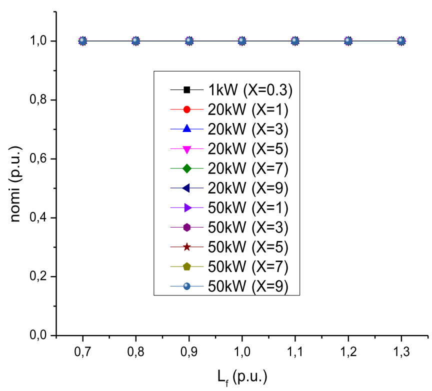

FIGURE 14. *nomi* vs L_f.

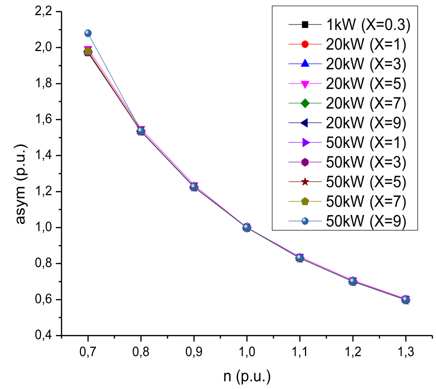

FIGURE 15. *asym* vs *n*.

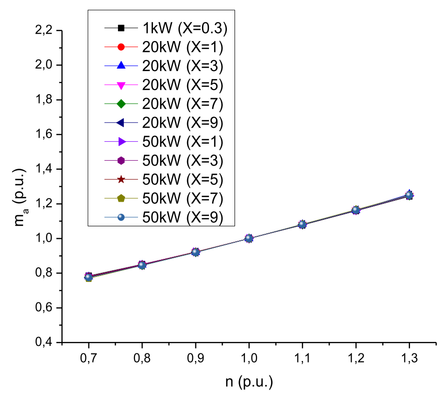

FIGURE 16. m_a vs *n*.

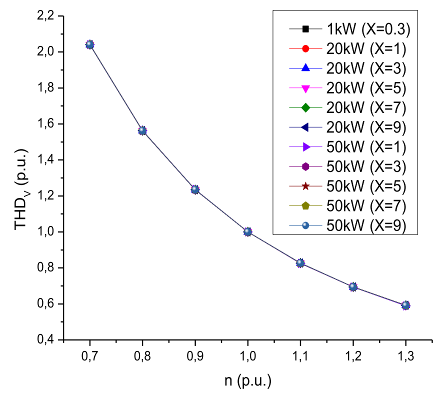

FIGURE 17. THD_V vs *n*.

reassures high power quality levels even under significant deviations (comparing to the optimal values) of the system parameters, special care has to be given to C_f capacitance selection. In this work, we considered a deviation between −30% and 30% of the optimized Cf value (shown in Table I). This is a reasonable assumption considering that the components can be affected by the operation conditions, the ageing of the materials and the component tolerances [36], [37] It is worth mentioning that for brand new components the component tolerance is the dominant factor, whereas for components in service ageing plays the most important role to the values changes. According to the presented results, it is shown that its unavoidable reduction over time [38]–[41] degrades significantly THD_V. Hence, it is recommended to keep THD_V target value (during the optimization procedure) at least 30% lower than the maximum acceptable limit, in order to be on the safe side. This safe precaution accounts also for any possible decrease of L_f inductance, as its effect on THD_V is significantly smaller than C_f affection. Nevertheless, if this precaution leads to inapplicable

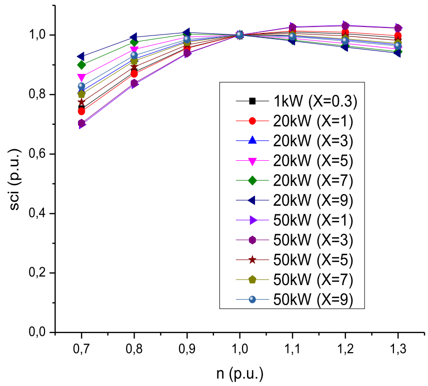

FIGURE 18. ***sci* vs *n*.**

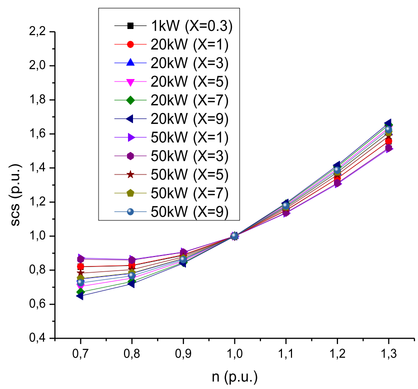

FIGURE 19. ***scs* vs *n*.**

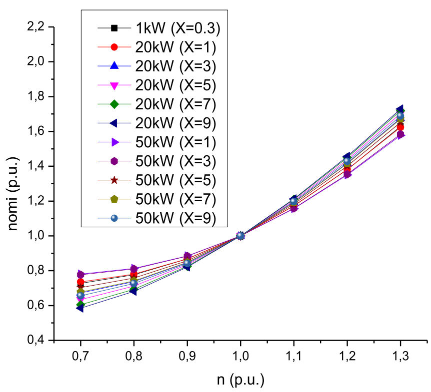

FIGURE 20. ***nomi* vs *n*.**

capacitance and/or inductance values, then the designer should consider the initial design utilizing higher tolerance capacitor solutions, i.e. metalized polypropylene film capacitors [42]. It is noted that the alterations of the capacitor series resistance are excluded from this analysis, due to the fact that polypropylene film or other types of capacitors with similar technical characteristics present very small dissipation factors [42].

In addition, the cautious selection and design of the filter capacitor bank (as it has been discussed) reassures also that *sci* and *scs* indices will be maintained below their predefined limits. Finally, it is noted that voltage asymmetry is going to

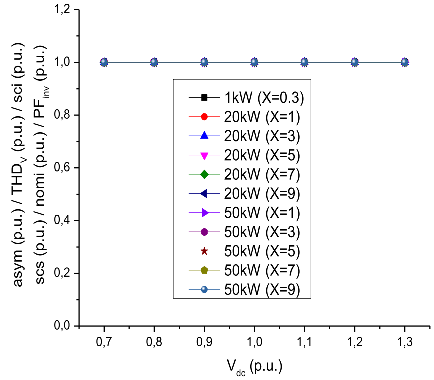

FIGURE 21. ***asym/THD$_V$ /sci/scs/nomi/PFinv* vs *V_{dc}*.**

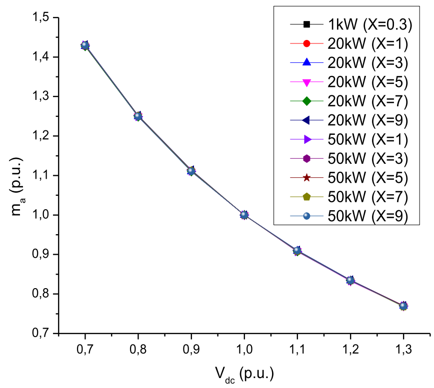

FIGURE 22. ***m_a* vs *V_{dc}*.**

TABLE 3. Behavior of each power quality index of each power quality index (↑increase, ↓decrease, - constant, ≈slight variation depending on *x*-value).

	C_f↑↓	L_f↑↓	n↑↓	V_{dc}↑↓
asym	↑↓	↑↓	↓↑	—
THD_v	↓↑	↓↑	↓↑	—
m_a	↓↑	↓↑	↑↓	↓↑
sci	↓↑	↓↑	≈	—
scs	↑↓	↓↑	↑↓	—
nomi	↑↓	—	↑↓	—

be positively affected over time, as a result of the expected reduction of C_f capacitance and L_f inductance.

Table 3 summarizes the sensitivity analysis results, indicating the behavior of each power quality index with respect to the parameters deviation of the standalone system.

IV. EXPERIMENTAL RESULTS

The theoretical calculations are evaluated by means of experimental (under scale) measurements. The laboratory configuration consists of the following components:

- a DC power supply, 0-330V/ 0-11A
- a set of iron core inductors 3×36mH, 30A

- a set of center tapped iron core inductors 3x5/10mH, 30A
- a three phase diode bridge rectifier, 510V/20A
- a three phase center tapped transformer, Ygd, 6 kVA, 50 Hz, 380 V / 110 V-220 V
- a film capacitor bank, 3×200 μF, 400 Vrms
- a film capacitor bank, 3×100 μF, 400 Vrms
- a film capacitor bank, 3×50μF, 400 Vrms
- a film capacitor bank, 3×47 μF, 400 Vrms
- a film capacitor bank, 3×40 μF, 400 Vrms
- a film capacitor bank, 3×5 μF, 400 Vrms
- an electronic load, 0-2.4 kW
- a three phase inverter prototype, 0-800 V_{DC}, 3×0-400 V_{AC}, 3 kVA
- various resistive load banks

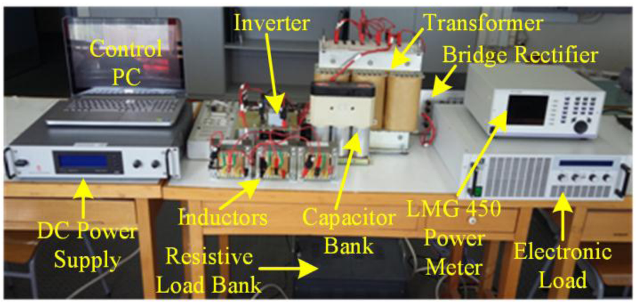

FIGURE 23. Laboratory setup.

Fig. 23 depicts the laboratory setup; note that the symmetrical load consists of a 3-phase diode H-bridge that supplies the resistive load bank at the dc side, whereas the variable (asymmetrical) load is the electronic one; $X = 0.3$ at 1 kW loading, while it changes linearly with the load active power.

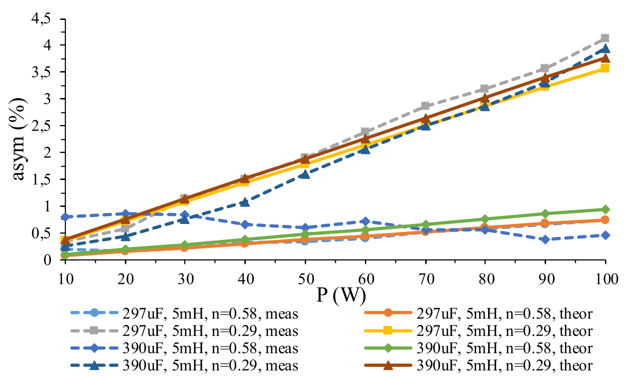

FIGURE 24. Experimental and theoretical *asym* results.

Figs. 24-28 depict the experimental results compared with the theoretical estimations as a function of the system parameters under study (C_f, L_f, n). More specifically, Fig. 24 presents the asymmetry analysis (under symmetrical load equal to 540 W) for different values of the parameters, while the single-phase non-symmetrical load varies from 10 W to 100 W. Figs. 25-28 depict the sensitivity analysis results

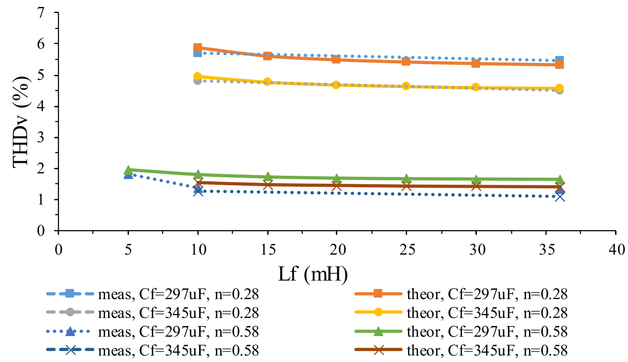

FIGURE 25. Experimental and theoretical THD_V results.

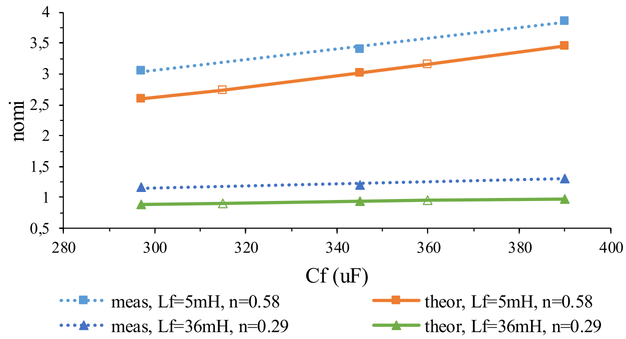

FIGURE 26. Experimental and theoretical *nomi* results.

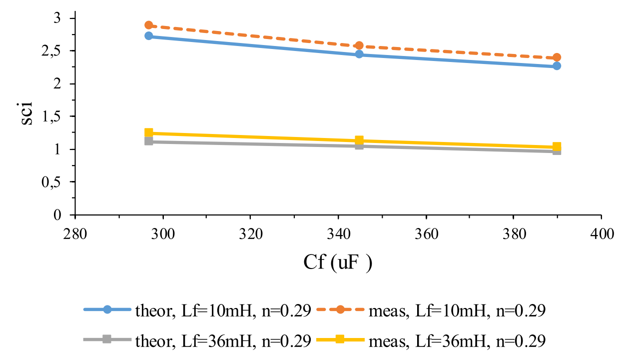

FIGURE 27. Experimental and theoretical *sci* results.

for the rest of the power quality indices, examining various scenarios for the parameters values. In more details, Fig. 25 presents THD_V as a function of the filter components and the transformer turns ratio. In Fig. 26, *nomi* variation is presented as a function of C_f and n, since it has no dependence on L_f changes. Fig. 27 depicts *sci* results, considering L_f and C_f variations, since the influence of n is not significant. Finally, Fig. 28 presents *scs* considering various combinations of C_f, L_f, and n values. The experimental results and theoretical calculations are in good match, confirming the dependence of each power quality index on the variation of the filter capacitance, the filter inductance and the transformer turns ratio. The deviation between the experimental and theoretical outcomes is mainly caused by the fact that the theoretical analysis ignors the power losses of the system (the efficiency

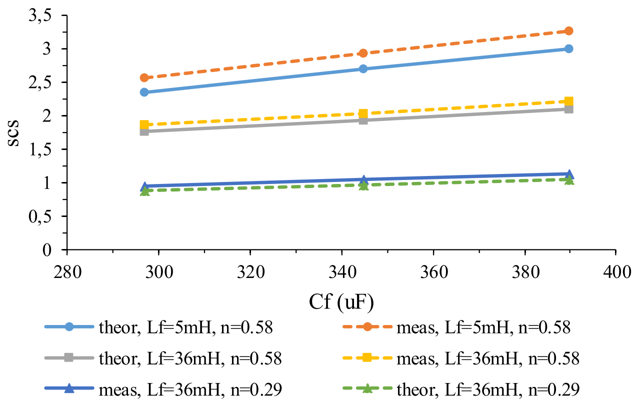

FIGURE 28. Experimental and theoretical *scs* results.

is considered equal to 1.0). Additionally, it is worth mentioning that even under symmetrical loading conditions, the load voltage is not free of asymmetry due to the unavoidable asymmetries among the filter inductors and the capacitors. However, even under such conditions, the experimental outcomes highlight that the voltage asymmetry remains well below its limit, as a result of the optimized design algorithm of the whole system according to [23].

V. CONCLUSIONS

The current work investigates the power quality of three phase standalone PV installations. The appropriate design of these systems is critical for the improvement of their power quality. In previous works [21]–[23], a methodology for the optimal design of these installations with improved power quality has been developed, in order to meet the demands of the relevant standards and offer realistic design solutions. Even though this method consists a reliable and efficient way in order to comply with the power quality standards and design limitations, its outcomes cannot always be implemented in practice, due to the availability of commercial components. In addition, the nominal value of each parameter presents an unavoidable drift over time. In this context the developed methodology and the results of the performed sensitivity analysis can be leveraged by the design engineers which now have at their disposal an efficient tool for the design of a standalone PV that provides prominent effect on power quality issues. The findings of the performed analysis are significant for the design of new as well as for the upgrade of autonomous systems. The obtained results and conclusions encourage the design engineers to adopt a preventive approach during the initial design of the PV system, highlighting the impact of the variation of each parameter on the power quality and the appropriate dimensioning of the system.

REFERENCES

[1] Official Journal of the European Union. (Apr. 2009). *Directive 2009/28/EC of the European Parliament and of the Council of 23 April 2009 on the Promotion of the Use of Energy From Renewable Sources and Amending and Subsequently Repealing Directives 2001/77/EC and 2003/30/EC*. [Online]. Available: http://eur-lex.europa.eu/legal-content/EN/TXT/PDF/?uri=CELEX:32009L0028&from=EN

[2] European Renewable Energy Council. (Jan. 2004). *Renewable Energy Technology Roadmap 20% by 2020*. [Online]. Available: http://www.erec.org/fileadmin/erec_docs/Documents/Publications//Renewable_Energy_Technology_Roadmap.pdf

[3] K. Ardani *et al.*, "Non-hardware ('Soft') cost-reduction roadmap for residential and small commercial solar photovoltaics," Nat. Renew. Energy Lab., Golden, CO, USA, Tech. Rep. NREL/TP-7A40-59155, Aug. 2013. [Online]. Available: http://www.nrel.gov/docs/fy13osti/59155.pdf

[4] T. Ackermann, G. Anderssonb, and L. Södera, "Distributed generation: A definition," *Electr. Power Syst. Res.*, vol. 57, no. 3, pp. 195–204, Apr. 2001.

[5] L. Kurdgelashvili, J. Li, C.-H. Shih, and B. Attia, "Estimating technical potential for rooftop photovoltaics in California, Arizona and New Jersey," *Ren. Energy*, vol. 95, pp. 286–302, Sep. 2016.

[6] A. Molin, S. Schneider, P. Rohdin, and B. Moshfegh, "Assessing a regional building applied PV potential—Spatial and dynamic analysis of supply and load matching," *Ren. Energy*, vol. 91, pp. 261–274, Jun. 2016.

[7] J. Philip *et al.*, "Control and implementation of a standalone solar photovoltaic hybrid system," *IEEE Trans. Ind. Appl.*, vol. 52, no. 4, pp. 3472–3479, Jul./Aug. 2016.

[8] R. A. Shayani and M. A. G. de Oliveira, "A new index for absolute comparison of standalone photovoltaic systems installed at different locations," *IEEE Trans. Sustain. Energy*, vol. 2, no. 4, pp. 495–500, Oct. 2011.

[9] S. S. Lee, B. Chu, N. R. N. Idris, H. H. Goh, and Y. E. Heng, "Switched-battery boost-multilevel inverter with GA optimized SHEPWM for standalone application," *IEEE Trans. Ind. Electron.*, vol. 63, no. 4, pp. 2133–2142, Apr. 2016.

[10] R.-J. Wai, W.-H. Wang, and C.-Y. Lin, "High-performance stand-alone photovoltaic generation system," *IEEE Trans. Ind. Electron.*, vol. 55, no. 1, pp. 240–250, Jan. 2008.

[11] J. T. Bialasiewicz, "Renewable energy systems with photovoltaic power generators: Operation and modeling," *IEEE Trans. Ind. Electron.*, vol. 55, no. 7, pp. 2752–2758, Jul. 2008.

[12] N. Stretch and M. Kazerani, "A stand-alone, split-phase current-sourced inverter with novel energy storage," *IEEE Trans. Power Electron.*, vol. 23, no. 6, pp. 2766–2774, Nov. 2008.

[13] L. Wang and D.-J. Lee, "Load-tracking performance of an autonomous SOFC-based hybrid power generation/energy storage system," *IEEE Trans. Energy Convers.*, vol. 25, no. 1, pp. 128–139, Mar. 2010.

[14] H. E. Farag, M. M. A. Abdelaziz, and E. F. El-Saadany, "Voltage and reactive power impacts on successful operation of islanded microgrids," *IEEE Trans. Power. Syst.*, vol. 28, no. 2, pp. 1716–1727, Mar. 2013.

[15] X. Li, D. Hui, and X. Lai, "Battery energy storage station (BESS)-based smoothing control of photovoltaic (PV) and wind power generation fluctuations," *IEEE Trans. Sustain. Energy*, vol. 4, no. 2, pp. 464–473, Apr. 2013.

[16] F. Valenciaga and P. F. Puleston, "Supervisor control for a stand-alone hybrid generation system using wind and photovoltaic energy," *IEEE Trans. Energy Convers.*, vol. 20, no. 2, pp. 398–405, Jun. 2005.

[17] C. Wang and M. H. Nehrir, "Load transient mitigation for stand-alone fuel cell power generation systems," *IEEE Trans. Energy Convers.*, vol. 22, no. 4, pp. 864–872, Dec. 2007.

[18] H. Fakham, D. Lu, and B. Francois, "Power control design of a battery charger in a hybrid active PV generator for load-following applications," *IEEE Trans. Ind. Electron.*, vol. 58, no. 1, pp. 85–94, Jan. 2011.

[19] T. Hirose and H. Matsuo, "Standalone hybrid wind-solar power generation system applying dump power control without dump load," *IEEE Trans. Ind. Electron.*, vol. 59, no. 2, pp. 988–997, Feb. 2012.

[20] J. Rocabert, A. Luna, F. Blaabjerg, and P. Rodríguez, "Control of power converters in AC microgrids," *IEEE Trans. Power Electron.*, vol. 27, no. 11, pp. 4734–4749, Nov. 2012.

[21] C. A. Christodoulou, I. F. Gonos, and I. A. Stathopulos, "Estimation of the parameters of metal oxide gapless surge arrester equivalent circuit models using genetic algorithm," *Electr. Power Syst. Res.*, vol. 81, no. 10, pp. 1881–1886, Oct. 2011.

[22] I. F. Gonos and I. A. Stathopulos, "Estimation of multilayer soil parameters using genetic algorithms," *IEEE Trans. Power Del.*, vol. 20, no. 1, pp. 100–106, Jan. 2005.

[23] C. A. Christodoulou, N. P. Papanikolaou, and I. F. Gonos, "Design of three-phase autonomous PV residential systems with improved power quality," *IEEE Trans. Sustain. Energy*, vol. 5, no. 4, pp. 1027–1035, Oct. 2014.

[24] C. A. Christodoulou, N. P. Papanikolaou, and I. F. Gonos, "Power quality assessment for autonomous residential PV systems," in *Proc. 16th Int. Conf. Harmonics Quality Power (ICHQP)*, Bucharest, Romania, May 2014, pp. 650–654.

[25] C. A. Christodoulou, N. P. Papanikolaou, and I. F. Gonos, "Power quality analysis for 3-phase standalone photovoltaic installations: A case study," in *Proc. 9th Medit. Conf. Power Generat., Transmiss. Distrib. (MED-POWER)*, Athens, Greece, Nov. 2014, pp. 1–5.

[26] T. V. Thang, A. Ahmed, C.-I. Kim, and J.-H. Park, "Flexible system architecture of stand-alone PV power generation with energy storage device," *IEEE Trans. Energy Convers.*, vol. 30, no. 4, pp. 1386–1396, Dec. 2015.

[27] P. Pillay and M. Manyage, "Definitions of voltage unbalance," *IEEE Power Eng. Rev.*, vol. 21, no. 5, pp. 49–51, May 2001.

[28] A. von Jouanne and B. Banerjee, "Assessment of voltage unbalance," *IEEE Trans. Power Del.*, vol. 16, no. 4, pp. 782–790, Oct. 2001.

[29] *Motors and Generators*, NEMA Standards MG 1-1993, 1993.

[30] *Input Performance of ASDs During Supply Voltage Unbalance*, EPRI Power Electronics Applications Center, Palo Alto, CA, USA, 1996.

[31] *IEEE Recommended Practice for Electric Power Distribution for Industrial Plants*, ANSI/IEEE Standard 141-1993, (Red Book), 1993.

[32] *IEEE Recommended Practice for Electric Power Systems in Commercial Buildings*, ANSI/IEEE Standard 241-1990, (Gray Book), 1990.

[33] *IEEE Standard Test Procedure for Polyphase Induction Motors and Generators*, IEEE Standard 112, 1991.

[34] *Voltage Characteristics in Public Distribution Systems*, Standard EN 50160, Jul. 2004.

[35] *International Standard, Electromagnetic Compatibility (EMC)—Part3: Limits_Section2: Limits for Harmonic Current Emissions (Equipment Input Current <16 A Per Phase)*, 3rd ed., document IEC 61000-3-2, 2004.

[36] J. Hannonen, J. Honkanen, J.-P. Ström, T. Kärkkäinen, S. Räisänen, and P. Silventoinen, "Capacitor aging detection in a DC–DC converter output stage," *IEEE Trans. Ind. Appl.*, vol. 52, no. 4, pp. 3224–3233, Jul./Aug. 2016.

[37] R. Kötz, P. W. Ruch, and D. Cericola, "Aging and failure mode of electrochemical double layer capacitors during accelerated constant load tests," *J. Power Sour.*, vol. 195, no. 3, pp. 923–928, Feb. 2010.

[38] M. Godec, D. Mandrino, and M. Gaberšček, "Investigation of performance degradation in metallized film capacitors," *Appl. Surf. Sci.*, vol. 273, pp. 465–471, May 2013.

[39] M. Makdessi, A. Sari, and P. Venet, "Metallized polymer film capacitors ageing law based on capacitance degradation," *Microelectron. Rel.*, vol. 54, nos. 9–10, pp. 1823–1827, Sep./Oct. 2014.

[40] J. Flicker, R. Kaplar, M. Marinella, and J. Granata, "Lifetime testing of metallized thin film capacitors for inverter applications," in *Proc. IEEE 39th Photovolt. Specialists Conf. (PVSC)*, Tampa, FL, USA, Jun. 2013, pp. 3340–3342.

[41] J. Vodrazka, M. Horak, and K. Dusek, "Aging analysis of metalized film capacitors," in *Proc. 16th Int. Conf. Mechatronics-Mechatronika (ME)*, Brno, Czech Republic, Dec. 2014, pp. 648–651.

[42] S. A. Vishay. *Film Capacitors: General Technical Information*. Accessed: Sep. 20, 2017. [Online]. Available: http://www.vishay.com/docs/26033/gentechinfofilm.pdf

DIONISIS VOGLITSIS received the Diploma degree in electrical and computer engineering from the Democritus University of Thrace, Xanthi, Greece, and the M.Sc. degree in electrical engineering from the Technical University of Delft, The Netherlands. He is currently pursuing the Ph.D. degree in grid-tied inverters for distributed generation with the Electrical and Computer Engineering, Democritus University of Thrace.

His research interests include the analysis, design, simulation, and construction of dc/dc and dc/ac converters for use in renewable energy systems, waste heat recovery systems, aeronautics applications, and wireless power transfer applications.

Mr. Voglitsis is a member of the Technical Chamber of Greece.

NICK P. PAPANIKOLAOU (M'08–SM'10) received the Dipl.Eng. and Ph.D. degrees in electrical engineering from the University of Patras, Rion-Patras, Greece, in 1998 and 2002, respectively.

Prior to his academic career, he had been for several years with Hellenic Electric Energy Industry, where he was involved in European transmission and generation projects. He is currently an Assistant Professor with the Department of Electrical and Computer Engineering, Democritus University of Thrace, Xanthi, Greece. His research interests include power electronics, renewable energy exploitation, distributed generation, energy saving, electric vehicles, and power quality improvement.

Dr. Papanikolaou is a member of CIGRE and the Technical Chamber of Greece.

CHRISTOS A. CHRISTODOULOU received the Dipl.Eng. and Ph.D. degrees in electrical engineering from the National Technical University of Athens, Athens, Greece, in 2006 and 2010, respectively. He was a Post-Doctoral Researcher with the Department of Electrical and Computer Engineering, Democritus University of Thrace, Xanthi, Greece, under the IKY-Siemens Fellowship Program from 2013 to 2015. He is currently with Hellenic Distribution Network Operator. He is also a Lecturer (annual contract) with the Department of Electrical and Computer Engineering, University of Thessaly. He is the author and co-author of more than 40 papers in scientific journals and conference proceedings.

His research interests include high voltages, lightning protection, distributed generation, electrical installations, energy saving, power quality improvement, and electromagnetic compatibility.

DIMITRIS K. BAROS (S'16) received the Diploma degree in electrical and computer engineering from the Democritus University of Thrace in 2015, where he is currently pursuing the M.Sc. degree with the Electric Machines Laboratory.

His research interests include the analysis, design, simulation and construction of wireless power transfer systems and multilevel inverters for use in renewable energy systems, and aeronautical applications.

IOANNIS F. GONOS (S'01–M'03–SM'15) received the Dipl.Eng. and Ph.D. degrees in electrical engineering from the National Technical University of Athens, Athens, Greece, in 1993 and 2002 respectively.

He was a Researcher with the High Voltage Laboratory, National Technical University of Athens, from 2002 to 2013. He was a Laboratory Assistant with the High Voltage Laboratory and the Photometry Laboratory, National Technical University of Athens, from 1996 to 2013, the Hellenic Naval Academy from 1996 to 2001, and the Department of Energy Technology, Faculty of Technological Applications, Technological Education Institute of Athens, from 1996 to 2001. He has been a Lecturer with the School of Electrical and Computer Engineering, National Technical University of Athens, since 2013. His research interests include grounding systems, insulators, high voltages, measurements, electromagnetic compatibility, and genetic algorithms.

He has authored or co-authored over 130 papers in scientific journals and conferences proceedings. He is a member of CIGRE and the Technical Chamber of Greece.